ISBN: 978-3-95450-219-6 ISSN: 2226-0366 doi: 10.18429/JACoW-LINAC2024-THPB014

INTRABEAM SCATTERING SIMULATION WITH A NOVEL HYBRID-KINETIC MONTE CARLO METHOD FOR LINEAR ACCELERATORS

P. Desiré *,[1], A. Latina, CERN, Geneva, Switzerland
A. Gerbershagen, University of Groningen, Groningen, Netherlands
[1] also at University of Groningen, Groningen, Netherlands

Abstract

Recent studies have identified intrabeam scattering (IBS) as one of the processes that can have a significant impact on the beam dynamics of linacs with high-density and low-energy beams, such as in free electron sources (FELs), where IBS appears to be one of the effects that most limits their performance. Most existing simulation codes have been developed for circular lattices or assume Gaussian beams and thus cannot accurately simulate the desired scenario. Motivated by this problem, this work presents the implementation of IBS in RF-Track, a tracking code developed for linear accelerators. The numerical simulation follows a novel methodology based on a hybrid-kinetic Monte Carlo approach. The method has proven to be stable using different input parameters and has shown emittance and a Sliced-Energy-Spread (SES) growth in different scenarios, demonstrating the accuracy of the tool and making it a promising solution to understand SES growth in FELs.

INTRODUCTION

Intrabeam Scattering (IBS), which consists of particle-to-particle elastic collisions by Coulomb interaction, has been extensively studied due to its critical role in the performance of circular accelerators. IBS causes emittance growth in storage rings [1] and damping rings [2, 3], leading to a deterioration of their performance. Lately, it has also been shown to limit the efficiency of linear accelerators.

The latest photoinjector technologies have allowed free-electron laser light sources (FELs) to have much more dense beams, increasing the effect of IBS, which grows for low-energy and high-density beams. In fact, recent studies have shown that IBS can be a determining factor in the performance of these machines, as it causes a growth in the Sliced-Energy Spread (SES, also known as uncorrelated energy spread), which is a key parameter for efficient light production. SwissFEL obtained a SES of 15 keV with 200 pC bunches [4], whereas European XFEL found a value of 6 keV with 250 pC bunches [5]. Finally, the PhotoInjector Test facility at DESY Zeuthen, also for 250 pC bunches, measured 2 keV [6]. The mentioned results highly differ from the SES of around 1 keV predicted from simulations, which did not consider either Micro-Bunching Instabilities or IBS effects. For a better understanding of this problem, a simulation accounting for IBS is needed.

Most of the existing simulations are based on analytical descriptions of IBS, such as Piwinski's [7] or Bjorken and Mtingwa [8] formulations which assume Gaussian beams, an unrealistic approximation for the high-intensity and low-energy beams present in many linear accelerators. Some codes model the IBS effect based on a partial differential equation that describes the system evolution [2], but in this work, each collision is reproduced individually with a Monte Carlo (MC) method, aiming to maximize the accuracy. This idea has been exploited by the tracking codes MOCAC [9] and SIRE [10–12] for circular lattices and recently has been studied in linear architectures [13]. Our work builds on this idea, introducing a novel methodology: a hybrid-kinetic MC approach.

In this paper, the implementation of IBS in RF-Track [14], a tracking code developed for linear accelerators, is presented. The IBS effect was analyzed in two different proposed cases which showed the emittance and SES growth respectively. Both scenarios used different input simulation parameters to test the stability and convergence of the method.

IMPLEMENTATION

This section describes the logic followed by the proposed IBS algorithm, which follows a novel approach different from other Monte-Carlo-based implementations. Firstly, it is named "kinetic" because it calculates the force experienced by each macro particle in the bunch at each time step (dt) and applies it in the form of a thin kick. This is the standard approach used in RF-Track to compute and apply collective effects to the beam. Secondly, it is described as "hybrid" because the deflecting force is computed colliding each particle with an *average particle* obtained from a set of 3D meshes containing charge density, velocity, and temperature of the bunch in the 3D space. In particular, three 3D meshes are needed: one for the average velocity, one for the standard deviation of the velocity, and one for the charged density. Finally, the deflection angles are computed using an MC method where the Rutherford cross-section is used to resolve the kinematics of the interaction.

After creating the described 3D meshes, the algorithm iterates over all the particles in the bunch, applying the following three steps. The 3D meshes are updated at each IBS calculation.

* pdesirev@cern.ch

ISBN: 978-3-95450-219-6 ISSN: 2226-0366 doi: 10.18429/JACoW-LINAC2024-THPB014

Step 1: Average particle interpolation

The local average particle, q, is calculated first. The local average velocity, $\bar{v}$, and its variance, σ_v, are interpolated from the meshes using cubic interpolation. Then, the average particle's velocity, $\vec{q}_v$, is extracted randomly from a normal, Gaussian distribution:

$$\vec{q}_v \to N(\bar{v}, \sigma_v). \tag{1}$$

This accounts for the local temperature of the bunch. The local number density is directly interpolated from the charge mesh and, together with the particle's momentum, is moved to the $\vec{q}_v$ rest frame by a Lorentz boost.

Step 2: Computation of IBS parameters

The relevant kinematics for IBS can be computed in the rest frame of $\vec{q}_v$, which is considered the target particle. The first step is to compute the maximum impact parameter in the collisions, b_{max}, a key parameter in the simulation as it will be further discussed. As this quantity is transverse to the particles' motion, it is not affected by the relativistic frame change and can be computed directly in the lab frame.

The parameter b_{max} is calculated locally at the longitudinal location of the particle along the bunch, z. From a 2D mesh, the values $\text{Var}(X)$, $\text{Var}(Y)$ and their covariance $\text{Cov}(X,Y)$ are interpolated. Then, b_{max} is obtained as:

$$b_{\text{max}} = \left(\text{Var}(X)\text{Var}(Y) - \text{Cov}^2(X,Y)\right)^{1/4}. \tag{2}$$

The introduction of a local impact parameter reduces the sensitivity to tails that was observed when b_{max} was determined in terms of global σ_X or σ_Y, which is especially important in non-Gaussian beams. The covariance has been added to consider scenarios where $x-y$ coupling is present. The next step is to calculate the minimum scattering angle, θ_{min} [15]:

$$\theta_{\text{min}} = 2\arctan\left(\frac{q^2}{4\pi\epsilon_0}\frac{1}{2E_{\text{kin}}b_{\text{max}}}\right), \tag{3}$$

where E_{kin} is the kinetic energy of the particle in the $\vec{q}_v$ rest frame, q is the particle's individual charge, assumed to be the same for all particles of the bunch, and ϵ_0 is the vacuum permittivity. Then, the differential Rutherford cross-section is introduced [15]:

$$\frac{d\sigma}{d\Omega} = \left(\frac{q^2}{4\pi\epsilon_0}\right)^2\left(\frac{1}{4E_{\text{kin}}}\right)^2\frac{1}{\sin^4(\theta/2)}. \tag{4}$$

Eq. (4) shows that, firstly, the differential cross-section highly increases for small angles, which renders determinant the choice of b_{max}, and secondly, that the lower the energy of the beam, the more predominant IBS is. The total cross section is determined by integrating Eq. (4) over the solid angle between θ_{min} and π. Finally, once the total cross section determined and the local density in q_v rest frame (ρ) is known, the mean free path (λ) can be computed as follows:

$$\lambda = \frac{1}{\rho\sigma}. \tag{5}$$

Then, the average number of collisions expected is calculated by $N = dS/\lambda$, where dS is the step distance obtained from the time step (input parameter of the simulation, dt), as Eq. (6) shows:

$$dS = dt\beta c/\gamma. \tag{6}$$

Being β the relativistic factor of the particle. The division of γ appears from changing the time step to q_v rest frame, so it is the relativistic factor corresponding to this velocity.

We then define dS^*, the effective step length. Two possibilities are considered:

A) Less than one collision, $N < 1$. Then, dS^* is dS, such as in Eq. (6).

B) Many collisions, $N \geq 1$. Then, dS^* is λ. The collision, described in the following step, is then repeated N times.

Step 3: Collision

The last step is to compute the collisions. For each collision, two angles are extracted from random distributions:

- The azimuthal angle ϕ, obtained from a uniform distribution $U(0, 2\pi)$.
- The scattering angle θ, obtained by the CDF inverse method, taking as PDF the differential cross section in Eq. (4) multiplied by $\sin\theta$.

Then, a new momentum $\vec{p'}$ is computed as:

$$\vec{p'} = \left(|\vec{p}_0|\cos\theta,\ |\vec{p}_0|\sin\theta\cos\phi,\ |\vec{p}_0|\sin\theta\sin\phi\right),$$

where $\vec{p}_0$ is the initial momentum in $\vec{q}_v$ rest frame. Then, the code uses a 3D rotation to align the collision's outcoming direction with the momentum of the particle. Since RF-Track tracks macroparticles, not single particles, not all particles in a macroparticle are expected to scatter. A weight based on the exponential distribution function and the ratio of the mean free path and the integration distance was introduced:

$$w = 1 - \exp\left(-\frac{dS^*}{\lambda}\right), \tag{7}$$

where dS^* is the distance travelled by the macroparticle in the collision, which was discussed previously. The weight defined in Eq. (7) is used to calculate the new momentum, $\vec{p}_f$, of the macroparticle, as follows:

$$\vec{p}_f = \vec{p}'w + \vec{p}_0(1-w). \tag{8}$$

As mentioned in the previous step, the collision is repeated N times, a number which depends on the ratio between ds and λ. Note that N can be a non-integer; in that case, for the last collision, dS^* will be the decimal part multiplied by λ.

Once all collisions have been computed, the final momentum in Eq. (8) is boosted back in the lab reference frame. Finally, the momentum difference in the lab frame is computed, $\Delta\vec{p}_{\text{LAB}}$, allowing to calculate the equivalent force experienced by each macroparticle in the lab frame, as $\vec{F} = \Delta\vec{p}_{\text{LAB}}/dt$. This procedure is repeated for each particle in parallel.

ISBN: 978-3-95450-219-6 ISSN: 2226-0366 doi: 10.18429/JACoW-LINAC2024-THPB014

RESULTS

To test the developed method, a case in which the expected effect of IBS is relevant was studied. The contribution of IBS is expected to increase with the bunch charge and decrease with the emittance and the beam size [7], as well as with kinetic energy, as discussed. A test case characterized by the parameters of Table 1 was proposed. The tracking simulation was performed without IBS and secondly, with IBS using different time steps, dt. The results can be seen in Fig. 1, which shows a growth of a 1.2 % in a 0.2 m long drift in the 4D emittance due to IBS, with respect to the stable emittance found for the non-IBS case. In addition,

Table 1: Beam Characteristics to Model a Favorable IBS Case

Bunch charge	5.5 nC
Kinetic energy	10 MeV
Transversal normalized emittance ($\epsilon_\perp$)	0.1 mm
RMS of longitudinal coordinate (σ_z)	0.1 mm
RMS relative momentum spread (σ_P/P)	0.1%

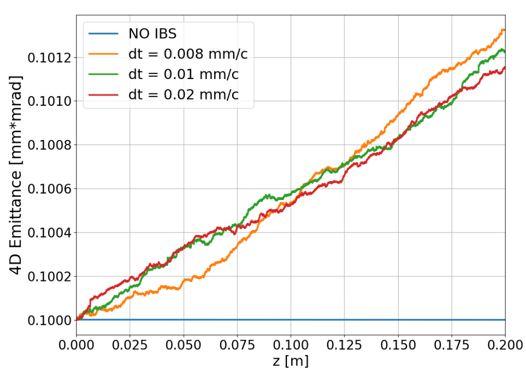

Figure 1: 4D Emittance growth along a 0.2 m drift with IBS, using different time steps, and without.

Fig. 1 proves the algorithm's stability, as different time steps predict almost the same emittance growth. The different fluctuations of the curves are due to the random nature of MC simulations; moreover, sampling in different step sizes will also result in kicks of different strengths (such as a random walk). However, convergence to the same result has been observed for all the cases, with a maximum uncertainty of around 0.0002 mm mrad along the trajectory. Figure 1 suggests that IBS affects not just the sliced energy spread but also the emittance growth. For example, the beam charge in Table 1, has been proposed for FCC-ee pre-injectors [16]. With such a high charge, even if the design emittances are bigger, the effect of IBS should be studied.

To study the effect of IBS on longitudinal beam dynamics, another case reproducing the beam conditions usually found in FELs, described in Table 2, was performed. A similar study was carried out, this time in a 5 m long drift. The results can be seen in Fig. 2, proving one more time the stability of the algorithm over different time steps and showing a SES growth of a 3 % in a 5 m long drift with respect to the case without IBS. However, the results do not include space-charge or MBI effects, which should be added in order to have a complete understanding of the SES growth in FELs.

Table 2: Beam Characteristics Typically Found on FELs

Bunch charge	300 pC
Kinetic energy	100 MeV
Transversal normalized emittance ($\epsilon_\perp$)	50 mm
RMS of longitudinal coordinate (σ_z)	1.25 mm
RMS relative momentum spread (σ_P/P)	0.02%

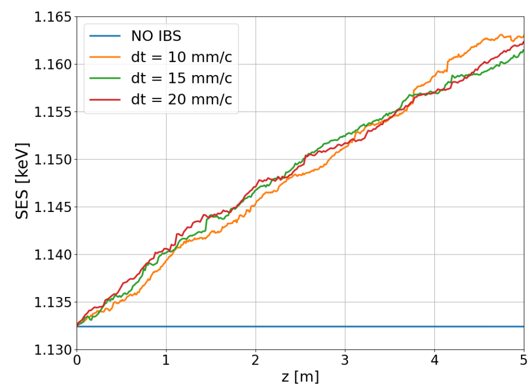

Figure 2: SES growth over a 5 m long drift, using different time steps in IBS simulation and without IBS.

CONCLUSIONS AND FUTURE WORK

A novel hybrid-kinematic MC method for IBS simulation in linear accelerators has been presented in detail. The algorithm features a multi-particle approach where each particle collides with a set of 3D meshes, capturing the bunch properties, including the local temperature. A test case in a region where the IBS effect was expected to be maximum was performed. The test showed a 1.2 % of transversal emittance growth in a 0.2 m long drift due to the IBS effect alone. Another test in a 5 m long drift replicating the usual beam characteristics found on FELs was carried out, finding a SES growth of 3 % caused by IBS.

The first tests of convergence over different time steps confirmed that the implementation is accurate and stable. In the immediate future, the code will need to be benchmarked against theory, other codes, and experimental results. Ultimately, the proposed tool will be used to study the effect of IBS in the FCC-ee pre-injector chain, where IBS is expected to be relevant due to the beam's high charge and low energy; in the muon collider's initial acceleration stage is also needed; and in photoinjectors, like those of FELs, aiming to find which part of the SES growth can be attributed to IBS effects.

ISBN: 978-3-95450-219-6 ISSN: 2226-0366 doi: 10.18429/JACoW-LINAC2024-THPB014

REFERENCES

[1] S. Papadopoulou, "Bunch characteristics evolution for lepton and hadron rings under the influence of the Intra-beam scattering effect", PhD Thesis, Univ. of Crete, Crete, Greece, 2019.

[2] M. Zampetakis *et al.*, "Interplay of space charge, intrabeam scattering, and synchrotron radiation in the Compact Linear Collider damping rings", *Phys. Rev. Acc. Beams*, vol. 27, p. 064403, Jun. 2024. `doi:10.1103/PhysRevAccelBeams.27.064403`

[3] F. Antoniou, "Optics design of Intrabeam Scattering dominated damping rings", PhD Thesis, Univ. of Athens, Athens, Greece, 2012.

[4] E. Prat *et al.*, "Energy spread blowup by intrabeam scattering and microbunching at the SwissFEL injector", *Phys. Rev. Accel. Beams*, vol. 25, p. 104401, Oct. 2022. `doi:10.1103/PhysRevAccelBeams.25.104401`

[5] S. Tomin *et al.*, "Accurate measurement of uncorrelated energy spread in electron beam", *Phys. Rev. Accel. Beams*, vol. 24, p. 064201, June 2021. `doi:10.1103/PhysRevAccelBeams.24.064201`

[6] H. Qian *et al.*, "Slice energy spread measurement in the low energy photoinjector", *Phys. Rev. Accel. Beams*, vol. 25, p. 083401, Aug. 2022. `doi:10.1103/PhysRevAccelBeams.25.083401`

[7] A. Piwinski, "Intra-beam-scattering", in *9th International Conference on High-energy Accelerators*, Stanford, CA, USA, May 1974, pp. 405-409. `doi:10.5170/CERN-1992-001.226`

[8] D. Bjorken, S.K. Mtingwa, "Intrabeam Scattering", *Part. Accel.*, vol. 13, pp. 115–143, 1983.

[9] P. Zenkevich, O. Boine-Frankenheim, A. Bolshakov, "A new algorithm for the kinetic analysis of intra-beam scattering in storage rings", *Nucl. Instrum. Methods Phys. Res.*, vol. 561, pp. 284-288, 2006.

[10] S. Papadopoulou *et al.*, "Impact of non-Gaussian beam profiles in the performance of hadron colliders", *Phys. Rev. Accel. Beams*, vol. 23, p. 101004, Oct. 2020. `doi:10.1103/PhysRevAccelBeams.23.101004`

[11] A. Vivori, M. Martini, "Intra-beam scattering in the CLIC Damping Rings", in *Proc. IPAC'10*, Kyoto, Japan, May 2010, paper WEPE090, pp. 3557–3559.

[12] M. Martini, F. Antoniou, Y. Papaphilippou, "Intrabeam scattering", *ICFA Beam Dyn. Newsl.* vol. 69, pp. 38-59, 2016.

[13] E. Gjonaj, "Intrabeam Scattering effects in the electron injector of the European XFEL", in *Proc. 40th Int. Free-Electron Laser Conf., (FEL'22)*, Trieste, Italy, Aug. 2022. `doi:10.18429/JACoW-FEL2022-WEP14`

[14] A. Latina, "RF-Track reference manual", Jun. 2020. `doi:10.5281/zenodo.4580369`

[15] J. Jackson, "Classical electrodynamics", New York: Wiley, 1999.

[16] P. Craievich *et al.*, "The FCCee Pre-Injector Complex", in *Proc. IPAC'22*, Bangkok, Thailand, Jun. 2022, pp. 2007–2010. `doi:10.18429/JACoW-IPAC2022-WEPOPT063`